MESH-BASED INTERPOLATION ON 2-MANIFOLDS

KEVIN SCULLY

Received 1 September 2004 and in revised form 20 December 2004

This paper presents a global L^1-estimate for the convergence of mesh-based interpolants on 2-manifolds defined over multiple coordinate systems and analyzes the convergence of an integral on a triangulated approximate manifold to the desired integral on the manifold being approximated. To place this estimate in context, previous convergence estimates for interpolation techniques on manifolds are presented. Finally, numerical results demonstrating the value of the L^1-estimate are presented.

1. Introduction

Mesh-based interpolation (e.g., finite-element interpolation) of functions defined on surfaces and manifolds has received attention in a diverse range of applications including computer graphics [3], structural engineering [5], and astrophysics [11]. In many of these applications, the domain in question possesses substantial curvature or discontinuities in its tangent plane and can only be described nonsingularly with multiple coordinate systems. In these scenarios, subtle details of approximation, unseen in the traditional framework, arise which may prevent convergence [2, 14].

To elucidate these details, this paper presents a global L^1-convergence estimate for mesh-based element interpolants on 2-surfaces (and 2-manifolds). To place this estimate in context, we offer a brief survey of efforts to construct interpolants on manifolds for Petrov-Galerkin methods. (A more thorough survey appears in [18].)

This survey will examine Nedelec's approach as described in [17] which has served as a standard for finite-element approximation across multiple coordinate systems. This survey will also discuss techniques not requiring a traditional mesh. These "meshless" methods provide context in two ways. First, they illustrate the use of global L^p-estimates, $1 \leq p < \infty$, on manifolds. We will place mesh-based methods into a comparable framework, in contrast to the L^∞- and local L^p-estimates traditionally used. Second, meshless methods which decompose a subset of R^n into a covering of open sets parallel the use of open coverings in a manifold representation.

Before reading the survey, note the following technical point. The majority of the methods on manifolds surveyed have been developed for 2-surfaces lying in R^3, which up to equivalence, do not encompass all 2-manifolds. For example, Nedelec, Sheng, and

International Journal of Mathematics and Mathematical Sciences 2005:7 (2005) 1067–1083
DOI: 10.1155/IJMMS.2005.1067

Hirsch specifically exploit the structure of a 2-surface in R^3 to build their framework. The central result of this paper, by contrast, is built only from the manifold structure of the 2-manifold and applies more generally. However, to address the motivating examples for this result, this paper focuses mainly on 2-surfaces lying in R^3.

1.1. Mesh-based approaches. The challenge in developing mesh-based approaches to approximation on manifolds lies in relating the viewpoints of classical differential geometry and numerical approximation. In classical differential geometry, the different coordinate systems (also called "patches" or "charts") are blended together via smooth "partition-of-unity" functions, which then permit the definition of globally defined quantities (e.g., integrals) via the patches. The smoothness of the partition functions require substantial overlap among their supports and these support sets will frequently not be polygonal. Mesh-based interpolation, by definition, however, requires a polygonal decomposition of the underlying set. Also, in practice, numerical methods on manifolds favor disjoint partitions of manifolds [1, 14] which correspond to piecewise constant, discontinuous partition-of-unity functions, and thus, lie outside the framework of classical, differential geometry.

One sees these assumptions of no overlap among the charts and polygonal chart sets in the work of Nedelec. Further, we see the use of global L^∞-estimates, in Nedelec's work and the work of Sheng and Hirsch, thereby circumventing the difficulties in defining global integration when the classical differential geometric framework does not apply.

1.1.1. Nedelec's work. Nedelec [17] delivered some of the first surface approximation error estimates. He begins with p patches, polygonal sets $\{S_i\}$ which, together with maps Φ_i, form the surface. The sets $\{S_i\}$ partition the manifold disjointly, that is, they intersect only at their boundaries. He triangulates each S_i and constructs on each triangle T of S_i an interpolant F_T from a space containing all polynomials up to degree k of the chart function Φ_i. He then stitches each F_T together to form a C^0-function Φ_{ih} on S_i which is locally differentiable on each T. For the greatest diameter h across each triangulation of each S_i, the following estimates hold:

$$\begin{aligned}
&\max_{i=1\cdots p}\sup_{x\in S_i}\left|\Phi_i(x)-\Phi_{ih}(x)\right| \le Ch^{k+1}\max_{i=1\cdots p}\sup_{x\in S_i}\left|D^{k+1}\Phi_i(x)\right|,\\
&\max_{i=1\cdots p}\sup_{x\in S_i}\left|D^l\Phi_i(x)-D^l\Phi_{ih}(x)\right| \le Ch^{k+1-l}\max_{i=1\cdots p}\sup_{x\in S_i}\left|D^{k+1}\Phi_i(x)\right| 1\le l\le k+1,
\end{aligned} \tag{1.1}$$

where $|\cdot|$ refers to the standard vector or matrix norm. Nedelec then asserts, for sufficiently small h, the existence of a homeomorphism ψ between this approximate surface and the original surface whose inverse associates to each point p on the original surface the point on the approximate surface intersecting the surface normal at p. Via ψ, the triangulation of the approximate surface becomes a triangulation of the original surface. He then proves that, for F_T and the function $\psi\cdot F_T$ from S_i to the original surface,

$$\begin{aligned}
&\sup_{x\in T}\left|\psi\cdot F_T(x)-F_T(x)\right| \le Ch^{k+1}\sup_{x\in T}\left|D^{k+1}\Phi_i(x)\right|\\
&\sup_{x\in T}\left|D(\psi\cdot F_T(x))-D(F_T(x))\right| \le Ch^{k}\sup_{x\in T}\left|D^{k+1}\Phi_i(x)\right|.
\end{aligned} \tag{1.2}$$

He then gives estimates for the determinants $J(\cdot)$ of the metrics formed by these chart functions:

$$\sup_{x\in T}\left|J(\Phi_i(x))-J(F_T(x))\right| \le Ch^k \sup_{x\in T}\left|D^{k+1}\Phi_i(x)\right|, \tag{1.3}$$

$$\sup_{x\in T}\left|J(\psi\cdot F_T(x))-J(F_T(x))\right| \le Ch^{k+1} \sup_{x\in T}\left|D^{k+1}\Phi_i(x)\right|. \tag{1.4}$$

Note that the existence of ψ increases the expected order of convergence from the standard interpolation framework. In the forthcoming [19], we will demonstrate that this faster estimate holds when $\|D^2\Phi_i\|_\infty$ is finite and the surface is tangent plane continuous.

1.1.2. Sheng and Hirsch. The engineering-inspired field of "parametric surface meshing" is devoted to mesh-based interpolation of functions on surfaces. The following theorem of Sheng and Hirsch (see [20]) represents one of the most often cited convergence theorems in this field and again, employs an L^∞-estimate.

Theorem 1.1. *Let $S(u,v)$ be a C^2-smooth parametric patch defined on $[a,b]\times[c,d]$. Let $T\in[a,b]\times[c,d]$ be an arbitrary triangle with vertices (A_1,A_2,A_3) in the parametric space, and let h be the maximal edge length of the triangle. Then, linear interpolant S_T of S such that $S_T(A_i)=S(A_i)$ satisfies*

$$\sup_{(u,v)\in T}||S(u,v)-S_T(u,v)|| \le \frac{2}{9}h^2(M_1+2M_2+M_3), \tag{1.5}$$

where $\|\cdot\|$ is the Euclidean R^3-norm and $M_1=\sup_{(u,v)\in T}\|\partial^2 S(u,v)/\partial u^2\|$, $M_2=\sup_{(u,v)\in T}\|\partial^2 S(u,v)/\partial u\partial v\|$ and $M_3=\sup_{(u,v)\in T}\|\partial^2 S(u,v)/\partial v^2\|$.

1.2. Non-mesh-based approaches. The preceding mesh-based approaches use L^∞-estimates and rest on classical C^k-differentiability. We will see that the chart functions and the related transition functions are better described by weak differentiability and Sobolev spaces, that is, $W^{k,p}$, the space of functions with weak derivatives up to order k lying in L^p. The following non-mesh-based estimates provide a framework more natural for weak differentiability and on a related note, global L^p-estimates, $1\le p<\infty$. The first set of estimates use an alternative formulation of weak differentiability via Fourier series.

1.2.1. Interpolation on manifolds via Fourier series. The interpolation of an $L^2(=W^{0,2})$- or $H^k(=W^{k,2})$-function on a manifold, given a sampling of its values (either measured under an integral sign or measured pointwise after making assumptions to clarify the almost everywhere ambiguity of L^2-functions), via the construction of interpolants based on Fourier series has been studied in the papers [8, 9, 16]. Often the interpolants are built from "radial basis functions" which vary only according to the radial distance from a fixed point [16]. With these Fourier series representations, the original functions and their interpolants are analyzed in terms of Sobolev spaces built from examining the decay of coefficients in the functions' Fourier series. Many approximation results on spheres and tori have been developed in this framework.

Narcowich et al. [16] present error estimates for these Fourier-based interpolants. First, they truncate the Fourier series of the original function f to obtain a series f_L with

a finite number of terms. Then, they approximate the truncated series with an interpolant $I_{\Phi,X}(f_L)$ built from a kernel Φ and a discrete subset X of the original domain Ω. From this set X, we may derive a "mesh norm" $h := \max_{y\in\Omega} \min_{x\in X} d(x,y)$. This norm measures, through the metric $d(x,y)$ of Ω, the furthest distance a point in Ω may lie from a point in X. Under the assumption that $\text{card}(X) = O(h^{-n})$, where n is the dimension of Ω and $\text{card}(X)$ refers to the number of elements in X, they prove an estimate of the form

$$\left|\left|f - I_{\Phi,X}(f_L)\right|\right|_{\infty,\Omega} = O(h^{\sigma-n/2})\|f\|_w, \tag{1.6}$$

where σ measures the rate of decay of the coefficients of f and the w-norm measures these coefficients relative to certain "weights."

1.2.2. Meshless methods. Non-mesh-based interpolation techniques, such as those described above, have given rise to "meshless methods." These Petrov-Galerkin methods for discretizing systems of partial differential equations without a mesh seek to eliminate the burdensome storage and time requirements of managing a mesh. The challenge these methods face lies mainly in numerical integration. The bottleneck in using Petrov-Galerkin methods to solve PDEs lies in solving the large matrices produced by discretizations of the integrated "weak form" equations. To make computations feasible, these matrices must be sparse. To create sparse matrices, the functions used must have local support and the construction of local support requires a decomposition of the domain into smaller pieces. Thus, while many of these meshless methods do not use meshes for interpolation, they use meshes for integration. Other methods do not use polygonal meshes, but use structures comparable to meshes, such as a spherical decomposition of the domain to define integration. In general, meshless methods have been found to be less efficient than mesh-based methods [4]. In fact, the architects of one such method later incorporated the polygonal meshes into their previous framework to avoid the difficulties caused by the lack of such a mesh [6, 7].

Among the meshless methods, two methods, in particular, lay theoretical groundwork for finite-element (and more generally, mesh-based) methods on manifolds. Both the partition-of-unity method [15] and the hp-cloud method [6] construct interpolants from partitions of unity built from an open cover of the domain. The parallels between open covers of sets in R^n and open covers of manifolds make these two methods relevant to this discussion. In each method, a function is approximated locally and from these local approximations, a global approximation is produced via the partition of unity. The key difference between these methods lies in the number of open sets in the covering. The partition-of-unity method more closely relates to our work, but the similarity and simultaneous arrival of the hp-cloud method make this method worthy of our attention.

In the partition-of-unity method, there is not necessarily an a priori relationship between the number of "patches" (open sets) and the rate of the convergence or between the size of the patches and the rate of convergence. While such relationships may exist in implementations of this method, the underlying theory only assumes the existence of $\epsilon_1(i)$ and $\epsilon_2(i)$ which bound the approximations on each patch. These ϵ's alone control the rate of convergence in the first global estimate below. In the second estimate, $\epsilon_1(i)$ must converge to zero faster than the inverse of the diameter of the patch goes to infinity.

This requirement, however, does not impose a functional relationship between the two. Thus, the number of patches may be of $O(1)$ if the convergence of these $\epsilon(i)$'s to zero does not depend on the number of patches or the area of these patches. Here, we offer the central results underlying this method.

THEOREM 1.2 (Melenk and Babuska). *Let $\Omega \subset R^n$. Let $\{\Omega_i\}$ be an open cover of Ω such that each point in Ω lies in only at most M of the Ω_i. Let $\{\phi_i\}$ be a partition-of-unity subordinate to this cover such that there exist constants C_∞ and C_G such that*

$$||\phi_i||_{L^\infty(R^n)} \leq C_\infty, \qquad ||\nabla\phi_i||_{L^\infty(R^n)} \leq \frac{C_G}{\operatorname{diam}(\Omega_i)}. \tag{1.7}$$

Let $V_i \subset H^1(\Omega_i \cap \Omega)$ and $V = \sum_i \phi_i V_i$. Let $u \in H^1(\Omega)$. Suppose that for each i, there exists $v_i \in V_i$, $\epsilon_1(i)$ and $\epsilon_2(i)$ such that

$$||u - v_i||_{L^2(\Omega_i\cap\Omega)} \leq \epsilon_1(i), \qquad ||\nabla(u - v_i)||_{L^2(\Omega_i\cap\Omega)} \leq \epsilon_2(i). \tag{1.8}$$

Then, the function $u_{\mathrm{ap}} = \sum_i \phi_i v_i \in V \subset H^1(\Omega)$ satisfies

$$\begin{aligned} ||u - u_{\mathrm{ap}}||_{L^2(\Omega)} &\leq \sqrt{M} C_\infty \left(\sum_i \epsilon_1^2(i)\right)^{1/2} \\ ||\nabla(u - u_{\mathrm{ap}})||_{L^2(\Omega)} &\leq \sqrt{2M}\left(\sum_i \left(\frac{C_G}{\operatorname{diam}(\Omega_i)}\right)^2 \epsilon_1^2(i) + C_\infty^2 \epsilon_2^2(i)\right)^{1/2}. \end{aligned} \tag{1.9}$$

Thus, we expect the order of the global approximation to be that of the local approximation.

In contrast to the partition-of-unity method, the hp-cloud method explicitly creates the local approximation space and bounds the error in this local approximation space as a function of the size of the open sets. The hp-cloud method decomposes the domain into $O(h^{-n})$ open balls ω_α^h, with each set occupying an area of $O(h^n)$, where h is the maximum of the dilation parameters h_α of the affine maps which send the open balls to the unit ball. The local approximation spaces are constructed from the partition functions whose supports intersect the given patch and from the product of these partition functions with polynomials. An estimate measuring the difference between a function $u \in W^{p+1}(\Omega \cap \omega_\alpha^h)$ and its local interpolant $\Pi_\alpha^2 u$ is proven under comparable assumptions to those of the partition-of-unity method: each partition function satisfies $\|\phi_\alpha^h\|_{L^\infty(\Omega)} \leq C_\infty$ and $\|\nabla\phi_\alpha^h\|_{L^\infty(\Omega)} \leq C_G/h_\alpha$ and each point of Ω is contained in at most M charts. A simplified version of this estimate follows:

$$|u - \Pi_\alpha^2 u|_{m,2,\Omega\cap\omega_\alpha^h} \leq C_\alpha h_\alpha^{p+1-m} |u|_{p+1,2,\Omega\cap\omega_\alpha^h}, \tag{1.10}$$

where $m = 0, 1$. These local interpolants are then stitched together over the $N(h)$ charts via the partition of unity functions. This approach produces comparable estimates to

those of the partition-of-unity method:

$$\begin{aligned} \left|\left|u-u_{\mathrm{hp}}\right|\right|_{L^2(\Omega)} &\leq MC_\infty \max_\alpha C_\alpha h^{p+1}\|u\|_{H^{p+1}(\Omega)}, \\ \left|u-u_{hp}\right|_{H^1(\Omega)} &\leq \sqrt{2}M\max_\alpha \left(C_G C_\alpha + C_\infty C_\alpha\right)h^p\|u\|_{H^{p+1}(\Omega)}. \end{aligned} \tag{1.11}$$

Both these methods invoke a partition of unity to combine local approximations into a global approximation and their approaches provide insight into mesh-based approximations on manifolds. Recall, however, that classical partitions of unity often do not give rise to polygonal decompositions of the manifold. In such a case, an approximate partition of unity and an approximate polygonal decomposition of the manifold will be used. The question then arises of how well the triangulation approximates the manifold.

2. Comparing functions on different manifolds

2.1. Defining a metric. To measure the error in a mesh-based approximation of a function on a manifold, we must somehow evaluate the difference between the triangulated manifold and the manifold it approximates. We will call two manifolds M and N equal if there exist a cover of M, $\{C_i\}$, $C_i \subset R^n$, and a cover of N, $\{D_i\}$, $D_i \subset R^n$, and maps $\gamma_{M,i} : C_i \mapsto M$ and $\gamma_{N,i} : D_i \mapsto N$ such that for all i, $C_i = D_i$ a.e. and $\|\gamma_{M,i} - \gamma_{N,i}\|_{W^{k,p}(C_i)} = 0$. (The choice of $p = 2$ seems the most natural for a framework for solving PDEs, but $p = 1$ appears to be the most theoretical satisfying choice, per our discussion below.)

This notion of equivalence of manifolds suggests a way of judging when two manifolds are "close." M and N are approximately equal if they have comparable charts structures C_i and D_i, respectively, whose symmetric difference $C_i \Delta D_i$ is small, and associated maps $\gamma_{M,i}$ and $\gamma_{N,i}$ which are both well-defined and nonsingular on $C_i \cup D_i$, and whose difference is small in a $W^{k,p}$-norm. With this viewpoint for evaluating the difference between two manifolds, we may define a "metric" (topologically speaking, a pseudometric) for evaluating the difference between two functions on M and N. The crucial idea is that while $\gamma_{M,i}$ needs only to be defined on C_i for purposes of constructing M, its definition may be extended to areas of D_i not in C_i without difficulty. We propose to measure the difference between a function f on M and a function q on N via the following function:

$$d_{M,N}(f,q) = \sum_i \left|\left|\phi_{M,i} f\sqrt{g_M} - \phi_{N,i} q\sqrt{g_N}\right|\right|_{L^1(C_i\cup D_i)}. \tag{2.1}$$

(By an abuse of notation, we refer to f both as a function from $M \mapsto R$ and via a chart map as a function from $C_i \mapsto R$.) Here, $\phi_{M,i}$ and $\phi_{N,i}$ refer to partitions of unity on their respective manifolds and g_M and g_N are the determinants of the metrics of their respective manifolds. Observe that $d_{M,M}(f,q) = \|f-q\|_{L^1(M)}$. (We assume that the same charts and partition of unity are used in both treatments of M.) Further,

$$\left|\int_M f - \int_{M_h} f\right| \leq d_{M,M_h}(f, f_h). \tag{2.2}$$

We now have a means for measuring our approximation of a function f on a manifold. We will demonstrate that this approximation depends upon our ability to approximate the function f on each chart, our ability to approximate the partition of unity functions, and our ability to approximate the determinant of the metric which derives from our ability to approximate the manifold. This observation is the essence of Lemma 2.1 to follow.

The L^1-norm, as opposed to another L^p-norm, appears in the definition for several reasons. First, because transition functions and chart maps will not take infinite values, the derivatives of transition functions and chart maps should have finite L^1-norm. This claim will not necessarily hold true for the L^p-norm, $p > 1$. Also, $d_{M,N}$ reduces to the L^1-norm on M when $M = N$ and the use of the L^1-norm appears to offer better convergence compared to alternatives we have considered. If we replace L^1 with L^2, $d_{M,N}$ will not reproduce the L^2-norm when $M = N$. Additionally, with this definition, using the techniques of the proof of Lemma 2.1 below, the L^1-norm appears to give a better convergence estimate (although this difference may just be a product of number manipulation in our efforts to find the most appropriate measurement). We could also replace the L^1-norm with L^2-norm and take the square roots of the partition functions and the fourth roots of the metric determinants. While this choice reproduces the $L^2(M)$-norm when $M = N$, it appears to give a lower order estimate in the approximation of the partition functions. Finally, note that since the sets in question are of finite measure, we may bound the L^1-norms by multiples of the L^2-norms:

$$\|f\|_{L^1} \leq \|f\|_{L^2}\sqrt{mA}. \tag{2.3}$$

2.2. Local (one-chart) error estimates. In the following lemma, we will take a chart C of a 2-manifold M and approximate it with a triangulation D, one part of a global triangulated approximation M_h. We will then bound the individual terms in the sum in d_{M,M_h} in terms of the approximations of its component parts: the function f, the partition of unity function, and the square root of the metric determinant. These errors are taken over D, assuming that these functions are defined on areas of D outside of C. Extending these errors over all of D, instead of over all triangles in D completely contained in C, appears to give rise to better higher-order approximation.

In the following lemma, we place no explicit restrictions on the differentiability of M. We place implicit restrictions on M by assuming the metric determinant is in L^∞. Further, we implicitly restrict the differentiability of M by assuming that the chart sets have piecewise $W^{r,1}$ boundaries since these boundaries are defined by transition functions. We may assume that the chart maps of M lie in $W^{k_1,p}$, $k_1 > 1$, and the transition functions lie in $W^{k_2,p}$, $k_2 \geq 1$. We will see that the differentiability of these functions will influence the rates of convergence of the different terms in the following estimate.

Lemma 2.1. *Let $C \subset R^2$ be a single chart set, a bounded, connected set with a piecewise $W^{r,1}$ boundary, $r = 1$ or 2, of a 2-manifold M. Let C be approximated by a triangulated polygon D such that each boundary edge of D is the linear interpolant of a $W^{r,1}$-segment of the boundary curve of C. Thus, there exists a set of intervals $[a_j, b_j]$ partitioning the boundary of C into curve segments such that on each segment, the boundary of C is given by $w = z_j(u)$, $z \in W^{r,1}([a_j, b_j])$, where w is either the x- or y-coordinate and $u \in [a_j, b_i]$. We assume that*

C and D are contained in larger charts so that areas of D not in C are defined and that the Lebesque measure $m(C \cup D)$ is finite. Let h be the maximum of the edge lengths of the triangles in D. Let f be a function defined on M, ϕ a partition of unity function for a covering of M containing C, and g the determinant of the metric components. Let f_h, ϕ_h, and g_h be the respective approximations of f, ϕ, and g defined on D and 0 outside D. Assume that all functions and their respective approximations are bounded above, both in L^1 and L^∞-norms on $C \cup D$. Suppose there exists $\epsilon > 0$ which bounds $|g|$ and $|g_h|$ from below, that is, that both metrics are nonsingular. Assume that the number of boundary triangles is at most $O(1/h)$. Then, there exists a constant K such that the following estimates hold:

$$\begin{aligned}&\left|\left|\phi f\sqrt{|g|}-\phi_h f_h\sqrt{|g_h|}\right|\right|_{L^1(C\cup D)}\\&\quad\le K\left(||\phi-\phi_h||_{L^1(D)}+||f-f_h||_{L^1(D)}+|||g|-|g_h|||_{L^1(D)}+h^r\right).\end{aligned}\tag{2.4}$$

Proof.

$$\begin{aligned}&\left|\left|\phi f\sqrt{|g|}-\phi_h f_h\sqrt{|g_h|}\right|\right|_{L^1(C\cup D)}\\&\quad=\left|\left|(\phi-\phi_h)f\sqrt{|g|}+(f-f_h)\phi_h\sqrt{|g|}+\left(\sqrt{|g|}-\sqrt{|g_h|}\right)\phi_h f_h\right|\right|_{L^1(C\cup D)}\\&\quad\le\left|\left|(\phi-\phi_h)f\sqrt{|g|}\right|\right|_{L^1(C\cup D)}+\left|\left|(f-f_h)\phi_h\sqrt{|g|}\right|\right|_{L^1(C\cup D)}\\&\qquad+\left|\left|\left(\sqrt{|g|}-\sqrt{|g_h|}\right)\phi_h f_h\right|\right|_{L^1(C\cup D)}\\&\quad\le||\phi-\phi_h||_{L^1(C\cup D)}\|f\|_{L^\infty(C\cup D)}\left|\left|\sqrt{|g|}\right|\right|_{L^\infty(C\cup D)}\\&\qquad+||f-f_h||_{L^1(C\cup D)}||\phi_h||_{L^\infty(C\cup D)}\left|\left|\sqrt{|g_h|}\right|\right|_{L^\infty(C\cup D)}\\&\qquad+\left|\left|\sqrt{|g|}-\sqrt{|g_h|}\right|\right|_{L^1(C\cup D)}||\phi_h||_{L^\infty(C\cup D)}||f_h||_{L^\infty(C\cup D)}.\end{aligned}\tag{2.5}$$

Now, for the sake of simplicity, we will replace these L^∞-norms with a constant K:

$$\begin{aligned}&\left|\left|\phi f\sqrt{|g|}-\phi_h f_h\sqrt{|g_h|}\right|\right|_{L^1(C\cup D)}\\&\quad\le K\left(||\phi-\phi_h||_{L^1(C\cup D)}+||f-f_h||_{L^1(C\cup D)}+\left|\left|\sqrt{|g|}-\sqrt{|g_h|}\right|\right|_{L^1(C\cup D)}\right)\\&\quad\le K\left(||\phi-\phi_h||_{L^1(C-D)}+||f-f_h||_{L^1(C-D)}+\left|\left|\sqrt{|g|}-\sqrt{|g_h|}\right|\right|_{L^1(C-D)}\right.\\&\qquad\left.+||\phi-\phi_h||_{L^1(D)}+||f-f_h||_{L^1(D)}+\left|\left|\sqrt{|g|}-\sqrt{|g_h|}\right|\right|_{L^1(D)}\right).\end{aligned}\tag{2.6}$$

And since all of the functions in question are bounded from above in $L^\infty(C \cup D)$, the preceding quantity is

$$\begin{aligned}&\left|\left|\phi f\sqrt{|g|} - \phi_h f_h \sqrt{|g_h|}\right|\right|_{L^1(C\cup D)} \\ &\quad \le K\left(\|1\|_{L^1(C-D)} + ||\phi - \phi_h||_{L^1(D)} + ||f - f_h||_{L^1(D)} + \left|\left|\sqrt{|g|} - \sqrt{|g_h|}\right|\right|_{L^1(D)}\right)\end{aligned} \tag{2.7}$$

(1 is the unit constant function)

$$\begin{aligned}&K\left(\|1\|_{L^1(C-D)} + ||\phi - \phi_h||_{L^1(D)} + ||f - f_h||_{L^1(D)} + \left|\left|\sqrt{|g|} - \sqrt{|g_h|}\right|\right|_{L^1(D)}\right) \\ &\quad = K\left(m(C-D) + ||\phi - \phi_h||_{L^1(D)} + ||f - f_h||_{L^1(D)} + \left|\left|\sqrt{|g|} - \sqrt{|g_h|}\right|\right|_{L^1(D)}\right).\end{aligned} \tag{2.8}$$

$C - D$ consists of regions formed where the boundary curves of C wander outside the triangles. Since we have assumed each edge of D is the piecewise linear interpolant of a boundary curve, we have

$$m(C-D) \le \sum_j \int_{[a_j,b_j]} |\, d_j(v) - \pi_h(d_j)(v)\,|\, dv. \tag{2.9}$$

Here $\pi_h(d_j)$ is the linear interpolant of d_j, that is, $d_j(a_j) = \pi_h d_j(a_j)$ and $d_j(b_j) = \pi_h d_j(b_j)$. (Note that the above sum also includes $D - C$.) Also, $(v,u) = (x,y)$ or (y,x) where (x,y) is the coordinate system of C_i, that is, u and v vary from triangle to triangle depending on whether it makes more sense to describe y as function of x or vice versa. From interpolation theory, we have

$$\int_{[a_j,b_j]} |\, d_j(v) - \pi_h(d_j)(v)\,|\, dv \le Kh^r \int_{[a_j,b_j]} \left|\, d_j^{(r)}\,\right| dv, \tag{2.10}$$

and since $|d_j^{(r)}|$ is bounded in integral,

$$m(C-D) \le \sum_j Kh^r(b_j - a_j) \le \sum_j Kh^{r+1}, \tag{2.11}$$

and since the number of j is $O(1/h)$,

$$m(C-D) \le Kh^r. \tag{2.12}$$

We now turn to the approximation of the square roots of the metric determinants. Observe

$$\left|\sqrt{|g|} - \sqrt{|g_h|}\,\right| = \frac{\left|\,|g| - |g_h|\,\right|}{\left|\sqrt{|g|} + \sqrt{|g_h|}\,\right|} \le \frac{1}{2\sqrt{\epsilon}}(|g| - |g_h|). \tag{2.13}$$

Incorporating the above inequality and (2.12) into (2.8) completes the proof. □

Corollary 2.2. *Suppose that C is polygonal, that is, that C may be triangulated exactly and $D = C$. Then $C \cup D = D = C$ and the h^r term may be removed from the preceding estimate. (In this case, we will most likely use the same partition function and the term involving partition functions may also be removed.)*

2.3. Global estimates. By summing the local estimates, chart by chart, into a global result, we obtain the following theorem.

Theorem 2.3. *Let M be a 2 manifold covered by charts $\{C_i\}$, with piecewise $W^{r,1}$, $r = 1$ or 2, boundary curves, with associated partition of unity functions $\{\phi_i\}$. (This may be an almost everywhere partition; that is, the partition of unity equations may fail on a set of measure 0.) For each i, let D_i be a triangulation of C_i such that each boundary edge of D_i is the linear interpolant of a $W^{r,1}$ boundary curve of C_i. Assume that the chart maps to M from C_i have a well-defined, one-to-one extension to $C_i \cup D_i$. Let M_h refer to the manifold defined by $\{D_i\}$ and the approximate chart maps. Let f be a function on M and g the metric. Let $\phi_{h,i}$, f_h, and g_h be local approximations to ϕ_i, f, and g, respectively. Assume that the metric determinants are bounded away from zero. (We will also use f_h to refer to the function on M_h which locally equals f_h.) Let h be a parameter which bounds from above, within a constant, the lengths of the sides of the triangles in each D_i. Let J refer to the number of C_i for which $m(C_i - D_i) > 0$. Then, the following estimate holds:*

$$d_{M,M_h}(f, f_h) \leq K\left(\left(\sum_i \left(||\phi_i - \phi_{h,i}||_{L^1(D_i)} + ||f - f_h||_{L^1(D_i)} + |||g| - |g_h|\,||_{L^1(D_i)}\right)\right) + Jh^r\right). \tag{2.14}$$

Thus, to understand the rate of convergence of an approximate integral, we must analyze the rate of convergence of each term in the estimate. For each respective term, we ask ourselves the following questions.

(1) What is the partition of unity? In the absence of an exact partition of the chart into triangles, the convergence of the partition of unity term is generally given by the smoothness of the transition functions.
(2) What interpolation scheme approximates f?
(3) Does the faster convergence of the inequality (1.4) apply? More specifically, does the surface have L^∞-bounded second derivatives of the chart to surface maps and a continuous tangent plane? If not, what is the differentiability of the chart maps? (A generalization of (1.4) to weakly differentiable chart maps appears in [19].)
(4) What is the differentiability of the boundary of each chart, that is, what is r? Like the convergence of the partition of unity term, this question depends on the smoothness of transition functions.

This estimate provides a framework by which we may evaluate approaches for approximating functions on manifolds. The work [18] examines several of these approaches in light of this framework, clarifying the limitations and underlying assumptions of such techniques. These approaches include the expression of a 2-dimensional, polygonal mesh in R^3 as a manifold by constructing charts out of all polygons containing a given vertex [10, 13] and manifold triangulation algorithms proposed by Kalik et al. [12] and Nedelec [17].

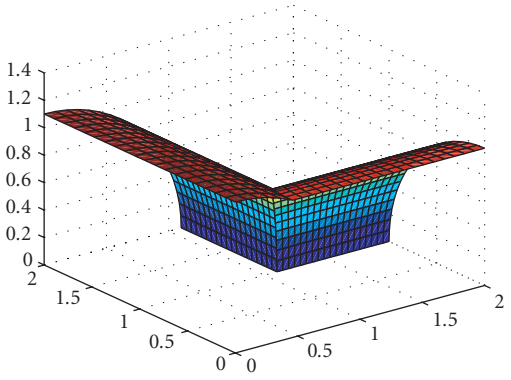

Figure 3.1. Two cylindrical patches.

Most approaches for triangulating a covering of a manifold will ignore the issue of overlap and gaps formed when triangulating each chart and treat the boundaries of each chart triangulation as if they align exactly. The partition of unity functions is generally ignored in such implementations, and by default, are taken to be the characteristic functions of their corresponding charts (i.e., a disjoint partition is used). The term $\|\phi_i - \phi_{i,h}\|$ is then bounded by the measure of the symmetric difference of C_i and D_i. Thus the accuracy of the triangulation in approximating the boundary curves, which come from the transition functions, bound this term. The partitions of unity term then depends on the smoothness of the transition functions and becomes equivalent to the Jh^r term.

3. Numerical examples

We examine some test cases in which we approximate an integral on a manifold by an integral on a triangulated approximation. In these examples, we do not explicitly construct a partition of unity and implicitly use characteristic functions as the partition of unity. When we do not have an exact partition, the differentiability of the boundary (via the Jh^r term) will dominate the convergence of the integral. When we have an exact partition, the differentiability of the chart to surface maps will govern convergence.

3.1. Two cylindrical patches. We consider the example (Figure 3.1) by Borouchaki and George [1]. The chart sets are "polygons" with straight edge boundaries except on their curve of intersection. The first surface patch is given by $\sigma_1(u,v) = (v, \cos u, \sin u)$ on the polygon given by $(\pi/2, 2)$, $(0,2)$, $(0,1.1)$, and $(\pi/2, \sqrt{.21})$. The second surface patch is defined by $\sigma_2(u,v) = (1.1\cos u, v, 1.1\sin u)$ on the polygon given by $(\pi/2, 0)$, $(\pi/2, 2)$, $(0,2)$, $(0,1)$, and $(\arcsin(1/1.1), 0)$. These patches intersect on the curve given by

$$\left(t, 1.1\sqrt{1 - \left(\frac{1}{1.1}\sin(t)\right)^2}\right), \quad t \in \left[0, \frac{\pi}{2}\right], \tag{3.1}$$

Table 3.1. $\int 1$ on Borouchaki and George's example.

h	Estimate	Error	Ratio
0.250000	4.840890	0.480487	—
0.125000	4.520969	0.160566	2.992459
0.062500	4.428000	0.067597	2.375348
0.031250	4.392062	0.031659	2.135134
0.015625	4.375801	0.015398	2.056101
0.007812	4.367988	0.007585	2.030061
0.003906	4.364149	0.003746	2.025010

in the first chart and

$$\left(t, \sqrt{1-\left(1.1\sin(t)\right)^2}\right), \quad t \in \left[0, \arcsin\left(\frac{1}{1.1}\right)\right], \tag{3.2}$$

in the second chart. Because this boundary curve between the charts is not piecewise linear, triangulations will only approximate the true chart sets.

Consider an approximation of the constant function $f = 1$ on this manifold. Because of the simplicity of this function and the fact that the metric is constant in each chart, the only obstacle to convergence to f in our metric is the convergence of the triangulated sets to the manifold. More specifically, $\int 1$ over the triangulated manifold will converge to $\int 1$ over the approximate manifold at the rate at which the piecewise, linear triangulated boundary converges to the curved boundary. Note that the boundary curve lies in $W^{1,1}$, that is, its first derivative is unbounded but bounded in integral. We, thus, expect the convergence of the integrals to be of $O(h)$, regardless of the degree of polynomial used. Our results in Table 3.1 confirm this prediction. Despite the fact that we use a quadrature scheme, precise on polynomials of degree three (called "precision 4 quadrature"), which ordinarily would produce $O(h^4)$ convergence, we still observe $O(h)$ convergence to the value of 4.360403.

3.2. The unit sphere. We extend the preceding example to the unit sphere. In the case $f = 1$, we know the integral to be 4π, the surface area of the unit sphere. Chart 1 is given by $\sigma_1(u,v) = (\cos(u)\cos(v), \sin(u)\cos(v), \sin(v))$, where $0 \le u \le \pi/2$ and $-\pi/3 \le v \le \pi/3$. The parametrization of chart 2 is given by $\sigma_2(\alpha,\beta) = (\sin(\alpha), \sin(\beta)\cos(\alpha), \cos(\beta)\cos(\alpha))$. Chart 3 is the same as chart 2, save that the third component is the opposite of the third component in chart 2. The boundary of chart 2 (likewise, chart 3) consists of the boundary curves $v = \pi/3$ (resp., $v = -\pi/3$) of chart 1, transformed into chart 2 coordinates, connecting the points $(0,\pi/6)$, $(\pi/6,0)$, $(0,-\pi/6)$, and $(-\pi/6,0)$. The curves $|\beta| = \arccos(\sqrt{3}/2\cos(\alpha))$ parametrize the boundary in both charts 2 and 3. Observe that these curves have an unbounded derivative which is bounded under the integral sign. Thus, this example resembles the first example in that the bounding curve is $W^{1,1}$-smooth and limits the convergence of any finite-element approximation to $O(h)$, as the results in Table 3.2 indicate. As before, because these boundary curves are $W^{1,1}$-smooth, we expect the convergence to be of $O(h)$.

Table 3.2. $\int 1$ on the unit sphere.

h	Chart 1	Chart 2	Chart 3	Total	Error	Ratio
0.250000	10.633021	0.718077	0.718077	12.069175	0.497140	—
0.125000	10.820567	0.769403	0.769403	12.359373	0.206942	2.402315
0.062500	10.867252	0.801894	0.801894	12.471040	0.095276	2.172040
0.031250	10.878911	0.820703	0.820703	12.520317	0.045999	2.071258
0.015625	10.881825	0.830922	0.830922	12.543670	0.022646	2.031241

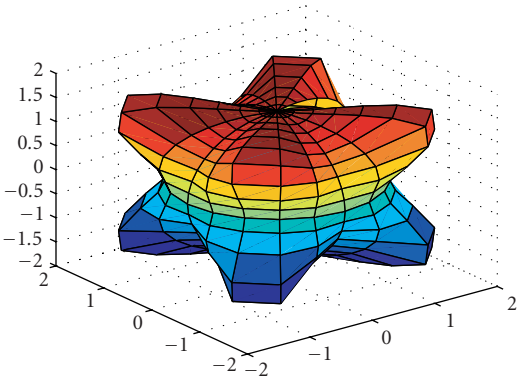

Figure 3.2. Fresnel's elasticity surface.

3.3. Fresnel's elasticity surface. This surface (Figure 3.2) appears in the study of optics and has the very complicated form $x = \lambda\cos(u)\cos(v)$, $y = \lambda\sin(u)\cos(v)$, and $z = \lambda\sin(v)$, where

$$\begin{aligned}\lambda = 1/\Bigg(&- 2\sqrt{0.965/3 - 0.935/3\big(\big(\cos(u)^4 + \sin(u)^4\big)\cos(v)^4 + \sin(v)^4\big)} \\ &\cdots\cos\Bigg(\Bigg(\arccos\Bigg(-\Big(-0.941/6 + 0.374\big(\big(\cos(u)^4 + \sin(u)^4\big)\cos(v)^4 + \sin(v)^4\big) \\ &\qquad - \cdots 1.309/6\big(\big(\cos(u)^6 + \sin(u)^6\big)\cos(v)^6 + \sin(v)^6\big) \\ &\qquad - 1.221\cos(u)^2\cos(v)^4\sin(u)^2\sin(v)^2\Big) \\ &\qquad /\cdots\Big(\sqrt{0.965/3 - 0.935/3\big(\big(\cos(u)^4 + \sin(u)^4\big)\cos(v)^4 + \sin(v)^4\big)}\Big)^3\Bigg) \\ &+ \pi\Bigg)/3\Bigg) + 0.8\Bigg).\end{aligned} \tag{3.3}$$

Table 3.3. Approximation of $\int 1$ on Fresnel's elasticity surface.

h	Error ratio
0.250000	11.972913
0.125000	4.652328
0.062500	2.822307
0.031250	2.111158

Because this surface is built from spherical coordinates, we expect and see similar convergence results to that of the sphere. Because of the difficulty in working with the complicated coordinate maps, direct analysis of these maps has been minimized. The discovery of singularities at $v = \pm\pi/2$ resulted from a numerical sampling script. The alternate parametrizations were constructed indirectly via the application of the above chart map to spherical transition functions. The metric components in different charts were constructed via finite-difference methods, avoiding differentiation of the above expression. Because we use the same spherical coordinates we used in the sphere example, the charts sets are exactly the same as for the sphere. Finally, the "correct integral," used to measure the error, results from a fine numerical approximation, given the difficulty of calculating the integral analytically. The results in Table 3.3 were obtained using "precision 3" quadrature.

3.4. Boundary convergence when $r = 2$. For the sake of completeness, we include two toy examples where, like the previous examples, the convergence of the trianglulated boundaries to the boundary curves of the charts dominates the convergence of the integral. In these two examples, however, the boundary curves lie in $W^{2,1}$ and thus the convergence progresses at $O(h^2)$ (corresponding to $r = 2$ in the Jh^r term).

In the first example, we consider a single chart set, given by the area bounded by the curves $y_b = \pm(x - x^{1.5})$. This boundary consists of an upper half and a lower half, both of which lie in $W^{2,1}$, but not in C^2. The chart map is just the function $\Phi(x, y) = (x, y, 0)$ and $f = 1$. Thus, the only obstacle to convergence is the boundary. Looping over $j = 1, \ldots, N - 1$ where $N \approx 1/h$, we form the rectangle from $x_j = j/(N + 1)$ to $x_{j+1} = j/(N + 1)$ and $-(y_b(x_j) + y_b(x_{j+1}))/2$ to $(y_b(x_j) + y_b(x_{j+1}))/2$, divide this rectangle into approximately N triangles (giving a total of $O(N^2) = O(1/h^2)$ triangles), and integrate. Note that this triangulation method violates the framework of our result in that each vertex of a triangle edge on the boundary does not interpolate a $W^{r,1}$-segment of y_b. However, the area of the difference between this crude triangulation and the one conforming to our framework is of $O(h^2)$ and thus, the convergence rates remain unchanged.

The second example closely resembles the first except that $y_b = \pm(x - x^4)$. This boundary curves consists of an upper half and a lower half, both of which lie in C^∞. However, as predicted by the theorem, we only witness $O(h^2)$ convergence. The results for this example and the previous example appear in Table 3.4.

3.5. $W^{k,1}$-surfaces. We examine a case where the smoothness of parametrization map, rather than the behavior of the transition functions or the approximated function, causes

Table 3.4. Boundary approximation when $r = 2$.

Boundary curves: $y = \pm(x - x^{1.5})$			
h	Estimate	Error	Ratio
0.125000	0.183244	0.016756	—
0.062500	0.194904	0.005096	3.287840
0.031250	0.198572	0.001428	3.567594
0.015625	0.199618	0.000382	3.739720
0.007813	0.199901	0.000099	3.841818
0.003906	0.199975	0.000025	3.902015
Boundary curves: $y = \pm(x - x^4)$			
h	Estimate	Error	Ratio
0.125000	0.550052	0.049948	—
0.062500	0.585028	0.014972	3.336101
0.031250	0.595878	0.004122	3.632601
0.015625	0.598917	0.001083	3.806036
0.007813	0.599722	0.000278	3.900246
0.003906	0.599930	0.000070	3.949402

the metric determinant approximation to slow the convergence. The following two-patch example uses a surface where the map from the chart to R^3 lies in $W^{k,1}$, but not in C^k. In the following example, the function being approximated is constant and the manifold is partitioned exactly, so that only the metric approximation term appears in the global convergence estimate.

Each chart set is the square $[0,1] \times [0,1]$. The first chart map is $\sigma_1(x,y) = (x^p + x, y, x^p + x)$. The second chart map is $\sigma_2(x,y) = ((x^p + x)(y^2 - 2y + 2), y - 1, (x^p + x)(y^2 - 2y + 2))$. This surface has continuous first derivatives across the mutual edge $y = 0$ in chart 1 and $y = 1$ in chart 2. For a positive integer p, the chart maps have bounded second derivatives. For $1 < p < 2$, the chart maps lie in $W^{2,1}$, as the chart map have unbounded second derivatives. Likewise, for $2 < p < 3$, the chart maps lie in $W^{3,1}$, as the chart map have unbounded third derivatives. The singularities of these derivatives behave like x^{p-2} for $1 < p < 2$ and x^{p-3}, for $2 < p < 3$ and occur on the line $x = 0$ in each chart.

We set $f = 1$. When the chart maps have bounded second derivatives, the inequality (1.4) governs convergence. When the second derivatives are unbounded, a modified version of (1.4) from [19] applies. For $p \geq 3$, we expect $O(h^{k+1})$ convergence where polynomials of degree k approximate the chart maps. For $1 < p < 2$, we expect $O(h^{k-1+p})$ convergence where $k \leq 1$. For $2 < p < 3$, we expect $O(h^p)$ convergence for $k \geq 2$ and $O(h^2)$ convergence if $k = 1$. Thus, we expect $O(h^p)$ convergence when we use a precision 2 quadrature rule on the metric determinant with $1 < p < 2$. We further expect that using quadrature rules of greater precision will not improve upon this convergence. The sampling of numerical experiments in Tables 3.5 and 3.6 confirms these hypotheses. We list the error ratios for different values of p, obtained on uniform triangulations of $[0,1] \times [0,1]$, along with the relevant prediction of the error ratio, for the given value of p. The ratios compare the error at $h = 0.031250$ to the error at $h = 0.015625$.

Table 3.5. Approximation of $\int 1$ on $W^{k,1}$-surfaces, precision 2 quadrature.

p	Error ratio	Predicted error ratio
1.1	2.1252	2.1435
1.2	2.2672	2.2974
1.3	2.4123	2.4623
1.5	2.6929	2.8284
2.2	3.9199	4
2.6	3.9860	4
3.0	4.0001	4

Table 3.6. Approximation of $\int 1$ on $W^{k,1}$-surfaces, precision 4 quadrature.

p	Error ratio	Predicted error ratio
1.1	2.1421	2.1435
1.2	2.2957	2.2974
1.3	2.4603	2.4623
1.5	2.8255	2.8284
2.2	4.5857	4.5948
2.6	6.0541	6.0629
3.0	16.0008	16

4. Conclusion

This paper has presented a new framework for measuring the convergence of mesh-based approximation of functions on 2-manifolds. This framework elucidates many of the subtle issues of approximation that present obstacles to existing mesh-based approaches. We hope this framework will bring a formalism which unifies our understanding of the many existing, ad hoc approaches to mesh-based approximation on manifolds and surfaces.

References

[1] H. Borouchaki and P.-L. George, *Delaunay Triangulation and Meshing. Application to Finite Elements*, Editions Hermès, Paris, 1998.

[2] H. Borouchaki, P. Laug, and P.-L. George, *Parametric surface meshing using a combined advancing-front generalized Delaunay approach*, Internat. J. Numer. Methods Engrg. **49** (2000), no. 1-2, 233–259.

[3] G. Celniker and D. Gossard, *Deformable curve and surface finite-elements for free-form shape design*, Comput. Graphics **25** (1991), no. 4, 257–266.

[4] S. De and K. J. Bathe, *The method of finite spheres*, Comput. Mech. **25** (2000), no. 4, 329–345.

[5] P. Destuynder and M. Salaun, *Approximation of shell geometry for non-linear analysis*, Comput. Methods Appl. Mech. Engrg. **152** (1998), no. 3-4, 393–430.

[6] C. A. Duarte and J. T. Oden, *An h-p adaptive method using clouds*, Comput. Methods Appl. Mech. Engrg. **139** (1996), no. 1-4, 237–262.

[7] ———, *H-p clouds—an h-p meshless method*, Numer. Methods Partial Differential Equations **12** (1996), no. 6, 673–705.

[8] N. Dyn, F. J. Narcowich, and J. D. Ward, *A framework for interpolation and approximation on Riemannian manifolds*, Approximation Theory and Optimization (Cambridge, 1996), Cambridge University Press, Cambridge, 1997, pp. 133–144.

[9] ———, *Variational principles and Sobolev-type estimates for generalized interpolation on a Riemannian manifold*, Constr. Approx. **15** (1999), no. 2, 175–208.

[10] M. Holst, *Adaptive numerical treatment of elliptic systems on manifolds*, Adv. Comput. Math. **15** (2001), no. 1-4, 139–191 (2002).

[11] M. Holst and D. Bernstein, *Adaptive finite element solution of the initial value problem in general relativity. I. Algorithms*, in preparation, 2002.

[12] K. Kalik, R. Quatember, and W. L. Wendland, *Interpolation, triangulation and numerical integration on closed manifolds*, Boundary Element Topics (Stuttgart, 1995), Springer, Berlin, 1997, pp. 395–417.

[13] A. Khodakovsky, P. Alliez, M. Desbrun, and P. Schroder, *Near-Optimal connectivity encoding of 2-manifold polygon meshes*, Graph. Models **64** (2002), no. 3-4, 147–168.

[14] K. Lin, *Coordinate-independent computations on differential equations*, Master's thesis, Massachusetts Institute of Technology, Massachusetts, 1997.

[15] J. M. Melenk and I. Babuska, *The partition of unity finite element method: basic theory and applications*, Comput. Methods Appl. Mech. Engrg. **139** (1996), no. 1-4, 289–314.

[16] F. J. Narcowich, R. Schaback, and J. D. Ward, *Approximations in Sobolev spaces by kernel expansions*, J. Approx. Theory **114** (2002), no. 1, 70–83.

[17] J. C. Nedelec, *Curved finite element methods for the solution of singular integral equations on surfaces in* R^3, Comput. Methods Appl. Mech. Engrg. **8** (1976), no. 1, 61–80.

[18] K. Scully, *Finite element approximation over multiple coordinate systems*, Phd thesis, University of California, San Diego, 2003.

[19] ———, *On* $W^{k,p}$*-manifolds and* $W^{k,p}$*-surfaces for analysis of the convergence of mesh-based approximation*, preprint, 2005.

[20] X. Sheng and B. E. Hirsch, *Triangulation of trimmed surfaces in parametric space*, Comput. Aided Des. **24** (1992), no. 8, 437–444.

Kevin Scully: The Aerospace Corporation, P.O. Box 92957, Los Angeles, CA 90009-2957, USA
E-mail address: kevin.j.scully@aero.org